JCTC Journal of Chemical Theory and Computation

Article

pubs.acs.org/JCTC

Density Fitting and Cholesky Decomposition of the Two-Electron Integrals in Local Multireference Configuration Interaction Theory

David B. Krisiloff,[†] Caroline M. Krauter,[‡] Francis J. Ricci,[†] and Emily A. Carter*[,‡,∥,¶]

Departments of [†]Chemistry and [‡]Mechanical and Aerospace Engineering, [∥]Program in Applied and Computational Mathematics, and [¶]Andlinger Center for Energy and the Environment, Princeton University, Princeton, New Jersey 08544, United States

Supporting Information

ABSTRACT: To treat large molecules with accurate ab initio quantum chemistry, reduced scaling correlated wave function methods are now commonly employed. Optimization of these wave functions in practice requires some approximation of the two-electron integrals. Both Cholesky decomposition (CD) and density fitting (DF) are widely used approaches to approximate these integrals. Here, we compare CD and DF for use in local multireference singles and doubles configuration interaction (LMRSDCI). DF-LMRSDCI provides less accurate total energies than CD-LMRSDCI, but both methods are accurate for energy differences. However, DF-LMRSDCI is significantly less computationally expensive than CD-LMRSDCI on the molecules tested, suggesting that DF-LMRSDCI is an efficient, often sufficiently accurate alternative to our previously reported CD-LMRSDCI method.

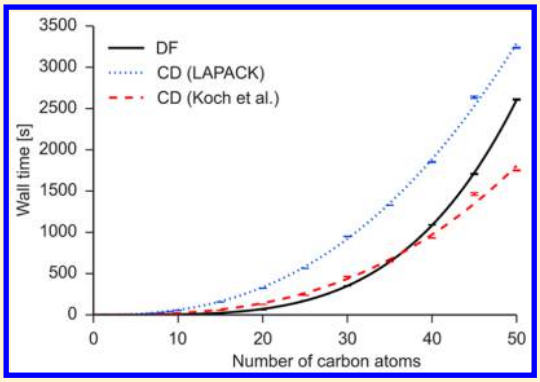

INTRODUCTION

Quantum chemistry has proven to be beneficial in both understanding experimentally observed phenomena and predicting novel behavior. The most accurate quantum chemical techniques for electronic structure problems are the so-called correlated wave function (CW) methods. The most common CW technique is coupled cluster (CC) theory;[1] the variant of CC theory that includes single and double excitations with perturbative triples (CCSD(T))[2] is often referred to as the "gold-standard" of quantum chemistry, at least for those molecules well described by a single reference state. Unfortunately, standard CCSD(T) scales as $O(N^7)$, where N is the number of basis functions. This unfavorable scaling makes the method computationally prohibitive for larger molecules. Other CW techniques, such as configuration interaction (CI)[3] and higher levels of Møller−Plesset (MP) perturbation theory,[3] have a similarly prohibitive computational scaling.

The $O(N^6)$ to $O(N^7)$ scaling of canonical CWs severely limits their application domain. The burdensome scaling can be attributed to two primary factors. First, the size of CWs does not grow linearly with molecular size. Second, solving for a canonical wave function requires evaluation of the two-electron integrals and their transformation from the atomic to the molecular basis, which is computationally expensive. Research into cheaper CW methods has focused on improvements in these two areas.

CW methods account for electron correlation by including excited electron configurations. The size of a CW therefore depends on the number of excited configurations included; computational cost can be reduced by removing some of these configurations. The local electron correlation approximation removes excitations for cases in which the orbitals involved are spatially far apart.[4] This is justified by the fact that electron correlation in nonmetallic systems decays quickly with distance as $1/r^6$. Therefore, removing configurations that involve orbitals distant from each other does not significantly alter the total wave function as their contribution to the total wave function would be small. The local electron correlation approximation was first employed by Pulay and Szabo[4−8] and is used in many different local CWs.[9−24] Other methods have also emerged to remove nonlocal correlations by nondistance metrics. The pair natural orbital (PNO) method, for instance, removes nonlocal correlations by creating a small set of unique, local virtual orbitals for each pair of internal orbitals.[25−27] The orbital-specific virtual method is similar to the PNO approach, though it creates a unique set of local virtuals for each individual internal orbital.[28] Instead of removing nonlocal excitations from the wave function, fragment-based methods construct the total wave function from the combination of the CWs of small fragments of the whole molecule. One of the earliest examples of this approach is the fragment orbital method.[29]

The two-electron integrals, consisting of two electrons in up to four orbitals, are denoted as

$$(ij|kl) = \int \frac{\phi_i(r_1)\phi_j(r_1)\phi_k(r_2)\phi_l(r_2)}{|r_1 - r_2|} dr_1 dr_2 \quad (1)$$

The ϕs are atomic orbitals (AOs), and r_1 and r_2 are the coordinates of electrons 1 and 2, respectively. We have assumed for convenience that the AOs are real valued. The two-electron integrals' computational expense arises from the number of

Received: August 7, 2015
Published: October 9, 2015

DOI: 10.1021/acs.jctc.5b00762
J. Chem. Theory Comput. 2015, 11, 5242−5251

integrals, which scales as $O(N^4)$, as well as the need to transform the integrals from the AO basis to the molecular orbital (MO) basis, which scales as $O(N^5)$. There are multiple approaches to reducing the cost of evaluating the two-electron integrals. We can avoid calculating blocks of near-zero integrals by using a Cauchy-Schwarz inequality.[30] Alternatively, integral estimates have been developed, which forsake the strict upper bound of Cauchy-Schwarz for a more accurate description of the two-electron integrals.[31−33] An additional way to reduce the cost of evaluating the two-electron integrals comes from exploiting linear dependencies among them. By decomposing the integrals, or equivalently, projecting them onto a more compact basis, we can rewrite the four-index integrals in terms of smaller, three-index quantities. Replacing four-index integrals with three-index quantities can typically, but not always, reduce algorithmic scaling. A number of different methods fall under this broad category. The pseudospectral (PS) method decomposes the two-electron integrals into analytic three-center, one-electron integrals and onto a spatial grid.[34−36] A pivoted, incomplete Cholesky decomposition (CD) can be used to decompose the two-electron integrals.[37−39] The resolution of the identity (RI) or density fitting (DF) methods both decompose the two-electron integrals onto an auxiliary basis set of atom-centered Gaussians.[40] Another promising approach views the two-electron integrals not as a matrix but as a fourth-order tensor. The tensor hypercontraction (THC) method decomposes the fourth-order, two-electron integral tensor using a standard tensor decomposition.[41] Different approximations for the Coulomb and exchange parts of the integrals have also been used. For example, in the chain-of-spheres exchange (COSX) method, the Coulomb part is approximated by a DF variant, while the exchange part is evaluated by seminumerical integration methods similar to the PS approach.[42]

The use of different two-electron integral decompositions for CW techniques has been widely studied. PS approaches have been explored for use in multiple methods, such as Hartree−Fock (HF), MP, and CI.[20,34−36,43−47] THC has been applied to various CC and CI methods.[48−51] DF and DF variants have become extremely popular and have been introduced to canonical, local, and explicitly correlated methods, to name just a few.[16,52−66] One of us previously compared the use of CD and atomic compact CD (acCD),[67] a DF method where the auxiliary basis is constructed on-the-fly using an atom-centered CD scheme, for local multireference singles and doubles configuration interaction (LMRSDCI).[68] While some recent studies compared the use of CD and DF for a number of methods including conventional CC,[69,70] CASSCF,[71] and symmetry-adapted perturbation theory (SAPT),[72] no research has been reported that incorporates DF into local (MR)SDCI. In this paper, we compare the use of DF and CD for LMRSDCI. First, we briefly discuss the CD and DF methods and our implementation of them. Second, we describe our LMRSDCI method, which uses the local electron correlation approximation and now either CD or DF for the two-electron integrals. Third, we determine the accuracy, total wall time, algorithmic, and parallel scaling of using CD and DF for LMRSDCI on a series of hydrocarbons. Finally, we demonstrate density-fitted LMRSDCI on a less-artificial test system by calculating the electronic component of the oxidation potential of a dinitroxide biradical.

THEORY

Cholesky Decomposition. Beebe and Linderberg first suggested using a CD to decompose the two-electron integrals in 1977.[37] In 2003, Koch et al. proposed a specific modification which then popularized the method (*vide infra*).[39] The CD decomposes a Hermitian, positive-definite matrix (V) into a lower triangular matrix (L) such that

$$V = LL^T \tag{2}$$

Using a column-wise approach, the elements of L can be calculated as

$$L_{b,b} = \sqrt{V_{b,b} - \sum_{c=1}^{b-1} L_{b,k}^2} \tag{3}$$

$$L_{a,b} = \frac{1}{L_{b,b}} \sqrt{V_{a,b} - \sum_{c=1}^{b-1} L_{a,c} L_{c,b}} \quad \forall\ a > b \tag{4}$$

Here, the indices a, b, and c refer to composite AO indices $\{ij\}$. However, the two-electron integral matrix, $V_{ij,kl} = (ij|kl)$, is not positive definite, but positive semidefinite. CD can be extended to these kinds of matrices through the use of pivoting. At each iteration b, the columns of the matrix V are pivoted such that $V_{b,b}$ is the largest remaining diagonal element, and the corresponding column is decomposed. The decomposition stops after $V_{b,b}$ falls below a numerical threshold. The size of L is $O(N_{bas}^2 N_{cho})$, where N_{bas} is the number of AO basis functions. N_{cho} is the number of decomposed columns of V, or equivalently, the number of columns of L, referred to as the number of Cholesky vectors. A two-electron integral can be computed from the decomposition in $O(N_{cho})$ time by

$$V_{ij,kl} = \sum_{P=1}^{N_{cho}} L_{ij}^P L_{kl}^P \tag{5}$$

Here, P indexes the Cholesky vectors. Moreover, note that eq 5 uses the common chemistry notation of placing the Cholesky/auxiliary index as a superscript and not a subscript.

Implementing a CD of the two-electron integrals involves one other consideration. Two-electron integrals are most efficiently calculated in blocks where all atomic basis functions belong to the same atomic shells. The integral $(ij|kl)$ is typically determined by calculating the block of integrals $(IJ|KL)$, where the AO i belongs to the atomic shell I, the AO j belongs to the atomic shell J, and so on. When using this approach to generate a single column of two-electron integrals, denoted as $(**|ij)$, multiple columns, denoted as $(**|IJ)$, are calculated. If we naively apply the CD algorithm, the other nonpivot columns in $(**|IJ)$ would usually be discarded, because the next pivot column is likely to lie within a different shell block. Koch et al. suggested partial pivoting in the CD to take advantage of being able to calculate multiple columns at once.[39] The Koch et al. algorithm calculates the diagonal integrals for picking pivots and then calculates the remaining two-electron integrals on-the-fly as follows. First, a new pivot is picked, as described above. Then, the columns $(**|IJ)$ containing the pivot are calculated, and the pivot column is decomposed. Second, an attempt is made to find a new pivot in the already calculated columns $(**|IJ)$, according to a modified criterion,[39] and the new pivot column is decomposed. The second step is repeated until there are no more acceptable columns in $(**|IJ)$ to decompose. Finally, the first step is repeated to find a new pivot among all the remaining columns of V. This approach tries to maximize the efficiency of integral calculation by avoiding the need to recalculate the columns $(**|IJ)$ multiple times for

DOI: 10.1021/acs.jctc.5b00762
J. Chem. Theory Comput. 2015, 11, 5242−5251

different pivots. However, the resulting decomposition tends to be less compact than a traditional CD due to the modified pivoting.

As an alternative to the Koch et al. implementation, two of us have recently proposed another approach for a CD of the two-electron integrals.[73] We calculate the entire two-electron integral matrix, after screening by the Cauchy-Schwarz criterion, and then decompose the matrix with the standard, fully pivoted CD. This approach results in a more compact decomposition, and we can take advantage of the high-performance LAPACK implementation of the fully pivoted CD.[74] However, we require more integral evaluations and have a higher storage demand; the Koch et al. approach only calculates columns of integrals as needed, while we calculate all columns. Since the decomposition ends before the entire matrix is decomposed, Koch et al. require fewer integral calculations. Both implementations have their merits, however. Depending on the overall CI algorithm, it may be more essential to have a faster CD (Koch et al.) or to have a more compact integral representation (our implementation). In our computer implementations of both algorithms, we have parallelized the integral calculation, but not the CD itself, with OpenMP. We will compare accuracy and timings for the partially pivoted Koch et al. and the fully pivoted LAPACK-based CD in the Results and Discussion section of this paper.

Density Fitting. In the DF approach, the two-electron integrals are expanded into an auxiliary basis of atom-centered Gaussians. Given N_{aux} auxiliary basis functions, a two-electron integral can be written as[40]

$$(ij|kl) \approx \Sigma_{PQ}^{N_{aux}}(ij|P)(P|Q)^{-1}(Q|kl) = \Sigma_{PQ}^{N_{aux}} C_{ij}^{P}(P|Q)C_{kl}^{Q} \tag{6}$$

The AO basis functions are i,j,k,l, and the conventional two-electron integral is $(ij|kl)$. P and Q index the auxiliary basis functions. $(ij|P)$ and $(Q|kl)$ are three-center two-electron integrals between two AO functions and one auxiliary function. Similarly, $(P|Q)$ is a two-center two-electron integral between two auxiliary functions. The C_{ij}^{P} are expansion coefficients calculated by solving the linear equation

$$\sum_{R} (P|R)C_{ij}^{R} = (P|ij) \tag{7}$$

As pointed out by other authors,[69] the expansion coefficients can easily be put into a form resembling a CD. If we contract the expansion coefficients with the square root of the two-center integrals, we obtain a new three-index quantity, B_{ij}^{P}:

$$B_{ij}^{P} = \sum_{Q} C_{ij}^{Q}(Q|P)^{1/2} \tag{8}$$

By inserting the definition of B_{ij}^{P} into eq 6, we can see that the formula for a two-electron integral becomes

$$(ij|kl) = \sum_{P=1}^{N_{aux}} B_{ij}^{P} B_{kl}^{P} \tag{9}$$

Eq 9 is functionally identical to the equation for a two-electron integral in a CD (eq 5), and the time to calculate such a two-electron integral scales as $O(N_{aux})$.

We solve for B_{ij}^{P} in the following manner. Eq 7 is a system of linear equations, which can be solved by a standard CD of the operator $(P|R)$. This results in two triangular linear systems that can be trivially solved. The CD of $(P|R)$ is also used as the matrix square root in eq 8. The final algorithm is as follows:

1. Calculate the matrix of $(P|Q)$ integrals.
2. Calculate $(P|Q)^{1/2}$ by CD.
3. Solve eq 7 using the result from step 2 and calculate the necessary $(P|ij)$ integrals, as needed.
4. Perform the final contraction, eq 8.

In our computer implementation of this algorithm, steps 3 and 4 are parallelized with OpenMP.[75] It is important to note that while steps 1−3 scale as $O(N_{bas}^2 N_{aux})$, step 4 scales as $O(N_{bas}^2 N_{aux}^2)$. Step 4 makes the DF functionally equivalent to a CD but is not required for general usage of DF. In principle, this implementation of DF should scale worse than the Koch et al. formulation of the CD.

The Three-Index AO to MO Transform. The Cholesky vectors or DF integrals need to be transformed to the MO basis for use in CI. This can be accomplished in two $O(N^4)$ steps instead of the canonical $O(N^5)$ algorithm. Starting from either eq 5 (CD) or eq 9 (DF), we denote the three-index quantity as $B_{\mu\nu}^{P}$. The transform to the MO basis can be written as

$$\widetilde{T_{\mu j}^{P}} = \sum_{\nu} C_{\nu j} B_{\mu\nu}^{P} \tag{10}$$

$$T_{ij}^{P} = \sum_{\mu} C_{\mu i} \widetilde{T_{\mu j}^{P}} \tag{11}$$

Here, μ and ν represent orbitals in the AO basis, i and j represent orbitals in the MO basis, and the columns of the C matrix represent the MOs. The final result, the three-index quantity in the MO basis, is T_{ij}^{P}. The quantity $\widetilde{T_{\mu j}^{P}}$ is an intermediate or half-transformed integral with one index in the AO basis and one index in the MO basis.

In our implementation of eqs 10 and 11, both equations are parallelized over the first MO index i with OpenMP. The additional memory required to store the intermediate, half-transformed $\widetilde{T_{\mu j}^{P}}$ is a necessary trade-off to reduce the algorithmic scaling. Eqs 10 and 11 appear to be independent of whether or not the $B_{\mu\nu}^{P}$ are Cholesky vectors or density-fitted quantities. However, the CD pivoting scrambles the order of the $\mu\nu$ pairs, and, as a result, the Cholesky vector transformation proceeds slightly differently. To minimize the impact of pivoting, we first transpose the Cholesky vectors so that each column is indexed by a $\mu\nu$ pair. In eq 10, accessing different columns becomes nonsequential, but elements within the column are accessed sequentially. Eq 11 proceeds identically for both the Cholesky vectors and density fitting.

Local Multireference Configuration Interaction and Averaged Coupled Pair Functional. Our local multireference configuration interaction algorithm has been discussed previously; therefore, here we only give a general summary.[22,24,73] The MRSDCI wave function can be written as

$$\psi_{MRSDCI} = \sum_{r} c_r \psi_r + \sum_{i,a} c_i^a \psi_i^a + \sum_{\substack{i\le j \\ a\le b}} c_{ij}^{ab} \psi_{ij}^{ab} \tag{12}$$

Each reference is denoted as ψ_r, single excitations from orbital i to orbital a are ψ_i^a, and double excitations from orbitals i,j to orbitals a,b are ψ_{ij}^{ab}. Each configuration has a corresponding coefficient, c, and the coefficient squared is the weight of the configuration in the overall wave function. We solve Schrödinger's equation, $H\psi_{MRSDCI} = E\psi_{MRSDCI}$, with Davidson's method.[76] Davidson's method avoids storing the entire Hamiltonian but requires the calculation of the matrix-vector product $\sigma = H * \psi$. We use the Symmetric Group Graphical Approach (SGGA) to handle the

DOI: 10.1021/acs.jctc.5b00762
J. Chem. Theory Comput. 2015, 11, 5242−5251

matrix-vector product.[77−80] To correct for the size-extensivity error in CI, we use the multireference averaged coupled-pair functional approximation 2 (MRACPF2).[81,82] MRACPF2 changes the eigenvalue equation being solved but is otherwise identical to the MRSDCI calculation. We use the Pipek−Mezey[83] technique to localize the internal orbitals and the local orthonormal virtual orbital (LOVO) method[84] for the virtual orbitals.

Once the local orbitals have been obtained, the local approximation to MRSDCI involves truncating double excitations, ψ_{ij}^{ab}, in two steps. First, we check if the internal orbitals i and j are spatially close. If they are not, then all double excitations from ij are neglected. This is the weak pairs (WP) approximation.[7] Second, we check if the virtual orbitals a and b are close to the internal orbitals. Again, if the virtual orbitals are spatially far apart from the internal orbitals, we truncate the double excitation. This is the truncation of virtuals (TOV) approximation.[7,12] We use a set of spheres to determine the distance between the two orbitals. We create a sphere for each orbital, representing the spatial distribution of the orbital. Each sphere encompasses the largest contributing atoms to each orbital, determined by contribution to the orbital's Mulliken charge. The sphere is centered at the mean position of the largest contributing atoms, weighted by their contribution to the Mulliken charge. If two spheres do not overlap, we then consider the two orbitals to be spatially far apart. The exact size of the spheres is independently tunable for the WP and TOV approximations. We have previously optimized these parameters for local MRACPF2 calculations.[85]

The three-index integrals, either Cholesky vectors or DF integrals, are used in the SGGA to compute the matrix-vector product. The SGGA is currently formulated in terms of the full four-index integrals, which we compute from the decomposed integrals in the following fashion. For the largest classes of integrals, those involving three or four virtual orbitals, we compute the integrals as needed, on-the-fly, during the SGGA. A Cauchy-Schwarz bound is used to avoid recalculating numerically insignificant integrals each time the SGGA is used. The smaller integral classes are computed before we begin Davidson's method and buffered.[86]

COMPUTATIONAL DETAILS

To benchmark the accuracy and efficiency of using DF in local MRSDCI, we have run a series of different calculations. If not stated otherwise, computations were carried out on nodes with two Intel Xeon E5-2670 @ 2.60 GHz processors with up to 128 GB of RAM. For the timing and accuracy comparisons, all geometry optimizations were performed at the Hartree−Fock (HF) level of theory with either Molcas 7.8[87] (the series of linear alkanes from C_1H_4 to $C_{30}H_{62}$) or ORCA[88] (all other structures). The orbitals used for single-reference calculations came from restricted HF (RHF), and the orbitals for multireference calculations came from complete active space self-consistent field (CASSCF) theory. The RHF and CASSCF computations were performed in Molcas 7.8[87] using CD with a threshold of 10^{-7}. In the case of multireference calculations, all configurations with a CASSCF weight larger than 0.01 were chosen as reference configurations in the subsequent LMRSDCI calculation, unless stated otherwise. For alkenes, alkynes, phenol, and cytosine, state-averaged CASSCF, including the ground state and one (or in the case of cytosine, three) excited state with equal weight, were used to obtain appropriately averaged orbitals for the LMRSDCI calculations of excitation energies. Unless stated otherwise, the correlation-consistent double-ζ basis set cc-pVDZ was used as the atomic basis set.[89] In the case of DF calculations, the corresponding auxiliary basis set cc-pVDZ-RI, optimized in the framework of DF-MP2, was chosen.[90,91] Note that the goal of the chosen approach is to analyze the differences in errors associated with different integral decomposition methods and not to obtain the most accurate possible results.

The determination of the oxidation potential of the dinitroxide biradical as a sample application of the newly implemented DF-LMRSDCI method required a set of geometry optimizations, some in the presence of an implicit solvent, which were performed in ORCA at the DFT-B3LYP/cc-pVDZ level of theory. Zero-point energies (ZPEs) and thermal (enthalpic and entropic) corrections were obtained with the standard harmonic oscillator, ideal gas, and rigid rotor approximations.[92] Where necessary, COSMO was used to implicitly include aqueous solvation. MOs were then generated using MOLCAS to perform restricted open-shell HF (ROHF) or CASSCF calculations (*vide infra*). We performed LMRSDCI computations using our TigerCI code. TigerCI generates the necessary integrals, both conventional and DF, with libint,[93] via ERKALE.[94,95] All steps for the redox application were done without a frozen-core approximation.

RESULTS AND DISCUSSION

In the following sections, we compare the accuracy and relative speed of using different CD algorithms and DF to handle the two-electron integrals. To distinguish between CI calculations with DF and CD, we denote CD calculations as either CD-LMRSDCI or CD-LMRACPF2 and DF calculations as DF-LMRSDCI or DF-LMRACPF2. In cases with a single reference we drop the MR, and in cases where there are a mix of single and multiple references we use (MR), i.e., CD-L(MR)SDCI. We compare the accuracy first for absolute energies and then for relative energies. Next, we compare the timings of the different two-electron integrals decompositions, followed by a discussion of the AO to MO transformation. We conclude by examining the timings for the entire calculation. Results for the parallel speedup and overhead can be found in the Supporting Information, Figures 1−6.

Accuracy. To compare the accuracy of using DF versus CD, we first compare total energies from a variety of different molecules. In general, the DF-L(MR)SDCI errors are much larger than the errors incurred by CD-L(MR)SDCI, regardless of the CD threshold. In Table 1, we compare the ground state total energies obtained from DF-L(MR)SDCI and CD-L(MR)SDCI

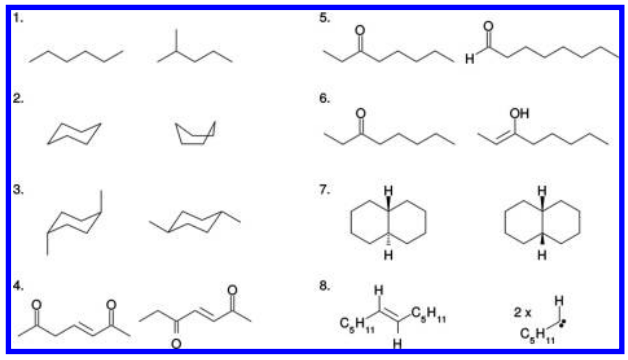

Figure 1. Set of molecules used for evaluating the accuracy of relative ground state energies obtained with DF and different CD algorithms. Adapted from ref 68.

DOI: 10.1021/acs.jctc.5b00762
J. Chem. Theory Comput. 2015, 11, 5242−5251

Table 1. Errors in Ground State Total Energies (in microHartree) for Some Linear Alkanes, Alkenes, and Alkynes, as well as Cytosine and Phenol, Obtained with DF and Different CD Algorithms, with Respect to L(MR)SDCI[a]

molecule	CD-L(MR)SDCI[b] (10^{-7}) [10^{-6}H]	CD-L(MR)SDCI[b] (10^{-5}) [10^{-6}H]	CD-L(MR)SDCI[c] (10^{-5}) [10^{-6}H]	CD-L(MR)SDCI[b] (10^{-4}) [10^{-6}H]	DF-L(MR)SDCI [10^{-6}H]
pentane[d]	0.3	22.1	20.7	−60.8	−3776.3
decane[d]	0.8	44.2	40.2	−754.0	−7383.9
pentadecane[d]	1.2	65.4	57.4	−1368.1	−10962.8
icosane[d]	1.7	83.2	74.1	−2087.5	−14527.8
3-*trans*-hexene[e]	0.2	20.3	18.5	−278.7	−4434.3
6-*trans*-dodecaene[e]	0.3	46.9	36.2	−1590.9	−8755.7
1-decyne[f]	0.8	32.5	32.0	−2520.3	−7351.2
1-pentadecyne[f]	1.3	21.0	18.5	−3623.6	−10929.1
1-icosyne[f]	2.1	−0.2	−1.1	−4437.0	−14485.3
phenol[g]	0.1	18.9	14.5	101.0	−5284.9
cytosine[h]	0.0	2.2	2.3	109.3	−0.9

[a]Benchmarks obtained by performing a CD-L(MR)SDCI calculation with the LAPACK-based decomposition and a CD threshold of 10^{-12}): $\Delta E = E$(CD/DF-L(MR)SDCI) − E(L(MR)SDCI). The CD thresholds are given in parentheses. Multireference calculations are marked as MR. [b]LAPACK-based fully pivoted CD scheme. [c]Partially pivoted scheme by Koch et al. [d]Single-reference calculation. [e]MR calculation; active space: 4 electrons in 4 orbitals (π, π^*,σ, σ^*). [f]MR calculation; active space: 4 electrons in 4 orbitals (all π/π^* orbitals) [g]MR calculation; active space: 8 electrons in 7 orbitals (all π/π^* orbitals) [h]MR calculation; active space: 14 electrons in 10 orbitals (all eight π/π^* orbitals + one oxygen and one nitrogen lone pair orbital); cutoff value for the weight of configurations from the CASSCF wave function: 0.05

to L(MR)SDCI. The reference values for L(MR)SDCI were generated by using a very tight CD threshold of 10^{-12} and the LAPACK-based CD algorithm. We compare errors engendered by different CD thresholds (10^{-7}, 10^{-5}, and 10^{-4}), as well as the two CD algorithms (Koch et al. and LAPACK-based). The DF approach yields relatively large errors for the ground state total energies, with the largest lying in the range of about 10^{-2}H (hartree). With a CD threshold of 10^{-7}, the errors are on the order of, or even smaller than, the energy convergence threshold of 10^{-6}H used during the L(MR)SDCI calculations. This implies that errors below 10^{-6}H are insignificant. We recommend a 10^{-7} CD threshold for high accuracy. With a CD threshold of 10^{-5}, the errors increase and are on the order of 10^{-5}H. The two different CD schemes, LAPACK-based (fully pivoted) and the one by Koch et al. (partially pivoted), yield almost the same results, so they can be used interchangeably as far as accuracy is concerned. As this is the case for all thresholds applied, we explicitly show the respective values from both algorithms only for a CD threshold of 10^{-5}. Finally, a CD threshold of 10^{-4} creates larger errors of up to 10^{-3}H, although these errors are still smaller than the errors for the DF scheme.

It is well-known that DF and CD yield larger errors for absolute energies than relative energies, where the latter are the ones needed for practical applications.[96] We therefore also compare relative ground state energies (Table 2) and valence electron excitation energies (Table 3). The molecule pairs used to estimate the errors in relative ground state energies are shown in Figure 1. This is the same set of molecule pairs one of us used in a previous publication to assess the accuracy of acCD, which is a method closely related to the DF scheme used here.[68] We have included the results from the aforementioned publication for comparison in Table 2. In acCD, the auxiliary basis functions for the DF calculation are generated on the fly from the AO basis using atomic CDs.[67,71,96−99]

DF-L(MR)SDCI errors in relative ground state energies are much smaller than for absolute energies (Table 2). The largest deviation is 0.41 kJ/mol (1.57×10^{-4}H) compared to L(MR)SDCI. Also, the errors are comparable to using acCD-L(MR)SDCI, which is not surprising given the close relationship between the two methods. Such errors on the order of a few 10^{-1}kJ/mol should be acceptable for most applications. As was the case for ground state total energies, the two CD algorithms employing different pivoting schemes yield almost the same errors, and the results from the partially pivoted algorithm are, again, only explicitly shown for a CD threshold of 10^{-5}. The deviations from L(MR)SDCI with a threshold of 10^{-5} are always smaller than the deviations by DF (by up to one order in magnitude). However, values obtained with a CD threshold of 10^{-4} yield relatively large errors (up to 3.68 kJ/mol = 1.40 mH) for the molecule pairs under consideration. It seems that the CD errors with very loose thresholds behave less systematically with respect to structural changes. We conclude that for reliable

Table 2. Errors in Relative Ground State Energies (in kJ/mol) of the Molecule Pairs Shown in Figure 1 with Different CD Algorithms and DF[a]

pair	L(MR) SDCI[b] energy difference	CD-L(MR) SDCI[c] (10^{-7})	CD-L(MR) SDCI[c] (10^{-5})	CD-L(MR) SDCI[d] (10^{-5})	CD-L(MR) SDCI[c] (10^{-4})	DF-L(MR) SDCI	acCD-L(MR) SDCI[e] (10^{-5})
1[f]	−0.69	0.00	0.00	−0.01	−0.24	−0.06	0.26
2[f]	28.81	0.00	−0.01	−0.01	−0.04	−0.02	−0.07
3[f]	−17.52	0.00	0.01	0.01	1.17	0.12	0.17
4[f]	−3.18	0.00	−0.02	−0.01	0.06	−0.10	0.01
5[f]	31.15	0.00	0.01	0.01	−1.91	0.18	0.06
6[f]	91.90	0.00	−0.02	−0.02	0.00	−0.05	−0.22
7[f]	12.78	0.00	−0.01	−0.01	−1.42	−0.08	−0.12
8[g]	704.05	0.00	0.02	0.02	−3.68	0.41	0.27

[a]The CD thresholds are given in parentheses. For reference, the relative ground state energies obtained with L(MR)SDCI are also shown. Multireference calculations are marked as MR. [b]Obtained using the LAPACK-based CD implementation and a CD threshold of 10^{-12}; relative energy between left and right structures as depicted in Figure 1, i.e., E(right)−E(left). [c]LAPACK-based and fully pivoted CD scheme, error with respect to L(MR)SDCI (10^{-12}). [d]Partially pivoted scheme by Koch et al.; error with respect to L(MR)SDCI (10^{-12}). [e]From ref 68; error with respect to L(MR)SDCI (10^{-12}). [f]Single-reference calculation. [g]MR calculation; active space: 4 electrons in 4 orbitals; dissociation to singlet carbene (supermolecule approach: two carbene molecules at approximately 20 Å distance).

DOI: 10.1021/acs.jctc.5b00762
J. Chem. Theory Comput. 2015, 11, 5242−5251

Table 3. Relative Errors of Valence Excited States (in eV) Obtained with Different DF and CD Schemes Compared to LMRSDCI[a]

molecule	state	LMRSDCI[b]	CD-LMRSDCI[c] (10^{-7})	CD-LMRSDCI[c] (10^{-5})	CD-LMRSDCI[d] (10^{-5})	CD-LMRSDCI[c] (10^{-4})	DF-LMRSDCI
3-*trans*-hexene[e]	$1^1\,\pi\,\pi^*$	8.132	0.000	0.000	0.000	−0.002	−0.002
6-*trans*-dodecaene[e]	$1^1\,\pi\,\pi^*$	8.242	0.000	0.000	0.000	0.003	−0.002
1-decyne[f]	$1^1\,\pi\,\pi^*$	8.016	0.000	0.000	0.000	0.000	0.000
1-pentadecyne[f]	$1^1\,\pi\,\pi^*$	8.062	0.000	0.000	0.000	0.001	0.000
1-icosyne[f]	$1^1\,\pi\,\pi^*$	7.083	0.000	0.000	0.000	0.002	0.000
phenol[g]	$1^1\,\pi\,\pi^*$	5.215	0.000	0.000	0.000	0.000	−0.001
cytosine[h]	$1^1\,\pi\,\pi^*$	5.742	0.000	0.000	0.000	−0.003	0.000
	$1^1\,n\,\pi^*$	5.817	0.000	0.000	0.000	−0.002	−0.001
	$2^1\,n\,\pi^*$	6.514	0.000	0.000	0.000	−0.002	0.000

[a]The CD thresholds are given in parentheses. For reference, the absolute values of the excitation energies obtained with LMRSDCI are also shown. [b]Obtained using the LAPACK-based CD implementation and a CD threshold of 10^{-12}. [c]LAPACK-based and fully pivoted CD scheme. [d]Partially pivoted scheme by Koch et al. [e]MR calculation; active space: 4 electrons in 4 orbitals (π, π^*,σ, σ^*). [f]MR calculation; active space: 4 electrons in 4 orbitals (all π/π^* orbitals). [g]MR calculation; active space: 8 electrons in 7 orbitals (all π/π^* orbitals). [h]MR calculation; active space: 14 electrons in 10 orbitals (all 8 π/π^* orbitals + one oxygen and one nitrogen lone pair orbital); cutoff value for the weight of configurations from the CASSCF wave function: 0.05.

reaction energies of the types of systems studied here and within our implementation of local MRSDCI, the CD threshold should be 10^{-5} or tighter.

Finally, we evaluate the errors in valence excitation energies (Table 3). The deviations obtained by DF do not exceed 0.002 eV (8×10^{-5} H), which again should be sufficient for most applications. As was the case for relative ground state energies, a CD threshold of 10^{-7} yields highly accurate results, while a CD threshold of 10^{-5} guarantees that the accuracy is not less than the DF accuracy and is therefore more than adequate. With a CD threshold of 10^{-4}, the results do not differ as much from DF as was the case for relative ground state energies, but the errors are still slightly larger than with DF in most cases. This affirms our choice to use CD thresholds of at least 10^{-5} in obtaining reliable results with our MRSDCI implementations for the classes of systems studied here.

In sum, despite large errors introduced by DF for ground state total energies, the influence on energy differences, such as excitation energies or relative ground state energies, are much smaller and do not affect the results significantly. With respect to accuracy, no significant deviations between the two CD algorithms introduced above (fully and partially pivoted) is observed. Also, we conclude that a CD threshold of at least 10^{-5} is necessary to guarantee the same accuracy with CD algorithms as with DF. Consequently, we used this threshold to obtain detailed timing information, which is presented in the next section. Note that much smaller CD thresholds have been shown to be accurate for CC.[69] While the accuracy of CD can be systematically improved by varying the CD threshold, the quality of DF calculations is determined by the predefined auxiliary basis set. The basis set used here has been initially optimized for DF-MP2 or DF-CC2 calculations. However, the small errors we obtain for our test set indicate that the basis set is sufficient for most applications in conjunction with LMRSDCI, too, and can be used without reoptimization. The same set of MP2-optimized auxiliary basis sets has also been successfully transferred to other methods like equation-of-motion CCSD[69] or CCSD with perturbative triples (CCSD(T)).[70] Note that we obtain similar results when using the cc-pVTZ basis set for higher accuracy (see the Supporting Information): very similar errors are obtained for the different schemes.

Timing. To understand the timing differences between DF-LSDCI and CD-LSDCI, we benchmarked both methods against a series of linear alkane chains. Alkane chains are pseudo-one-dimensional and represent a best case scenario for the local approximation. This makes them ideal molecules for examining the asymptotic behavior of new algorithms in local methods. Again, the CD threshold was set to 10^{-5} because it is the loosest threshold that guarantees errors no larger than those for the DF scheme. As previously mentioned, these calculations were performed using an integral-direct mode where the most expensive two-electron integrals are calculated on-the-fly rather than stored on disk (*vide supra*). The cost to calculate the integrals on-the-fly is a function of the decomposition strategy used. Therefore, the total timings provide a good measure of the effectiveness of the different decomposition algorithms.

First, we compare the time required to decompose the two-electron integrals, using either CD or DF. Figure 2 shows the wall time for different decomposition methods applied to linear alkane chains on eight cores. The different algorithms exhibit the expected scaling: the two CD algorithms scale as $O(N^3)$, while the DF scales as $O(N^4)$. The Koch et al. CD is faster than the LAPACK-based CD, as the Koch et al. CD algorithm requires significantly fewer integral evaluations. DF is the fastest

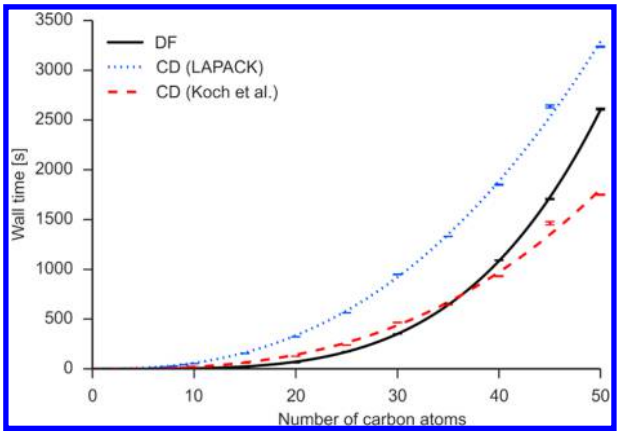

Figure 2. Dependence of the wall time for the integral decomposition on system size for linear alkane chains. Lines are fits of the wall time against $f(x) = ax^b$ with $a = 0.0006$ and $b = 3.92$ for the DF (black, solid line), $a = 0.19$ and $b = 2.49$ for the LAPACK-based CD (blue, dotted line), and $a = 0.03$ and $b = 2.78$ for the Koch et al. CD (red, dashed line). Plotted wall times are averaged over 10 values, and the error bars show the standard deviations.

DOI: 10.1021/acs.jctc.5b00762
J. Chem. Theory Comput. 2015, 11, 5242−5251

algorithm for relatively small molecules but because its cost grows faster than for CD, it becomes more expensive than the Koch et al. CD for relatively large molecules. We find that the exact location of the crossing point between the two methods is strongly dependent upon the number of threads used. For eight threads, DF becomes slower than the Koch et al. CD for alkane chains with more than 35 carbon atoms (Figure 2), while the crossing point lies at $C_{60}H_{122}$ when 16 threads are used (compare Figure 7 in the Supporting Information).

Although the LAPACK-based CD is slower than the Koch et al. CD, the LAPACK-based CD produces a more compact decomposition (Figure 3). However, the size difference is not

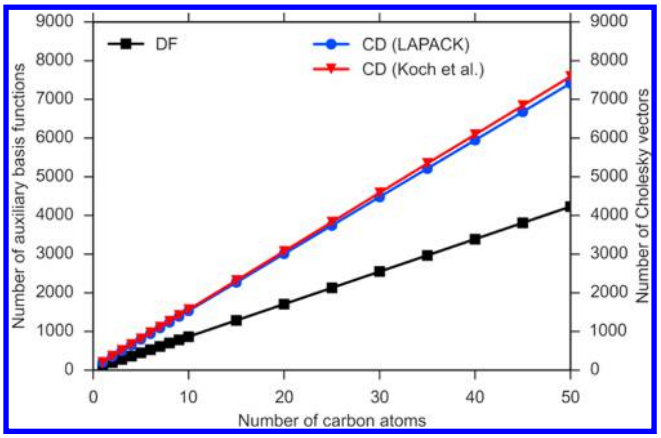

Figure 3. Number of Cholesky vectors (CD threshold: 10^{-5}) or auxiliary basis functions as a function of molecular size.

large, consisting of only a few hundred Cholesky vectors for the largest molecules tested (e.g., 175 fewer vectors for $C_{50}H_{102}$). By contrast, the number of DF auxiliary functions is significantly smaller than the number of Cholesky vectors (e.g., for $C_{50}H_{102}$ there are 3362 fewer auxiliary basis functions than LAPACK-based Cholesky vectors (fewer by a factor of 1.8)), although the difference depends on the CD threshold. At looser decomposition thresholds, the number of Cholesky vectors becomes comparable to the number of auxiliary functions. The difference between Cholesky vectors and auxiliary functions also manifests in the AO-to-MO transform (Figure 4). For any particular molecule, the smaller number of auxiliary functions compared to Cholesky vectors ensures that the DF transform is faster than the CD transform. The CD AO-to-MO transform also requires an additional transpose (*vide supra*), which also factors into the larger wall times. Note that the calculations with the Koch et al. CD for $C_{50}H_{102}$ had to be performed on a different node with more memory (node with two Intel Xeon E5-2670 v2 @ 2.50 GHz processors with up to 256 GB of RAM) because the AO-to-MO transformation exceeded the available memory on the nodes used for the rest of the data set by a few GB. Also, only two (instead of ten) runs were performed. Therefore, these results are not included in the determination of the scaling parameters.

The combination of differences in decomposition wall times, number of auxiliary functions/Cholesky vectors, and AO-to-MO transform times explains the differences in total wall times for the entire CI calculation (Figure 5). DF-LSDCI proves to be the fastest method due to a combination of faster decomposition and transform wall times, as well as a small number of auxiliary functions. The CD-LSDCI results show that the LAPACK-based CD and the Koch et al. CD are similar in speed, although the decomposition itself was faster for the Koch et al. CD. In this

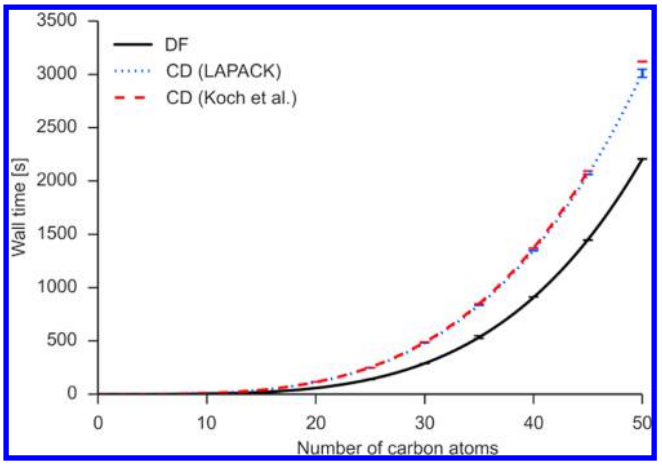

Figure 4. Dependence of the wall time for the AO-to-MO transformation on system size for linear alkane chains. Lines are fits of the wall time against $f(x) = ax^b$ with $a = 0.0004$ and $b = 3.98$ for the DF (black, solid line), $a = 0.002$ and $b = 3.60$ for the LAPACK-based CD (blue, dotted line), and $a = 0.002$ and $b = 3.60$ for the Koch et al. CD (red, dashed line). Plotted wall times are averaged over 10 values, and the error bars show the standard deviations. Exception: $C_{50}H_{102}$ with the Koch et al. CD is averaged over two runs only and omitted from the fit (run on nodes with up to 256 GB RAM).

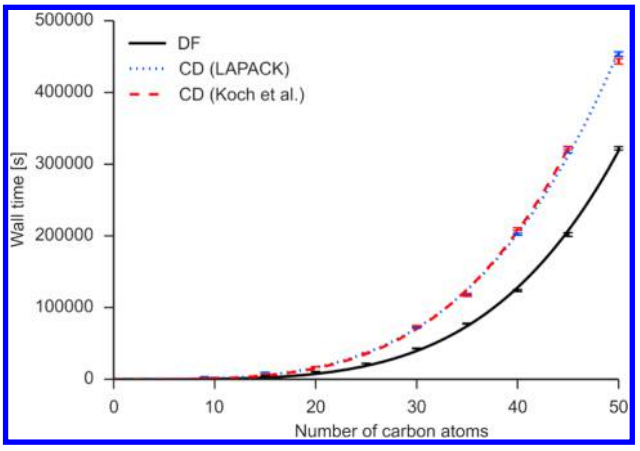

Figure 5. Dependence of the total wall time on system size. Lines are fits of the wall time against $f(x) = ax^b$ with $a = 0.04$ and $b = 4.09$ for the DF (black, solid line), $a = 0.3$ and $b = 3.64$ for the LAPACK-based CD (blue, dotted line), and $a = 0.2$ and $b = 3.76$ for the Koch et al. CD (red, dashed line). Plotted wall times are averaged over 10 values, and the error bars show the standard deviations. Exception: $C_{50}H_{102}$ with the Koch et al. CD is averaged over two runs only and omitted from the fit (run on nodes with up to 256 GB RAM).

instance, the smaller number of Cholesky vectors (LAPACK-based CD) gives a slightly faster run time after the initial decomposition step than the faster decomposition (Koch et al. CD). This result is likely dependent upon whether directly computed integrals are used. The number of Cholesky vectors affects the wall time less if the integrals are calculated once and then stored on disk than if the integrals are calculated on-the-fly multiple times. The overall scaling of all three methods is consistent with the worst scaling components being $O(N^4)$. Again, the results for $C_{50}H_{102}$ obtained with the Koch et al. CD are omitted from the determination of the scaling behavior with system size due to a different hardware setup and fewer runs performed (two instead of 10).

DOI: 10.1021/acs.jctc.5b00762
J. Chem. Theory Comput. 2015, 11, 5242−5251

The results presented here were obtained with the cc-pVDZ basis set and the corresponding auxiliary basis set cc-pVDZ-RI. For comparison, we have included data for a subset of the studied alkane chains with cc-pVTZ/cc-pVTZ-RI in the Supporting Information. The scaling of the DF and CD algorithms with system size is not significantly changed by increasing the basis set size.

Redox Application. We have demonstrated the effectiveness of DF-LMRSDCI on a set of relatively artificial test molecules. Here, we use DF-LMRSDCI on a more complicated chemical system, a dinitroxide biradical under investigation for potential antimicrobial properties (Figure 6).[100] We choose this molecule

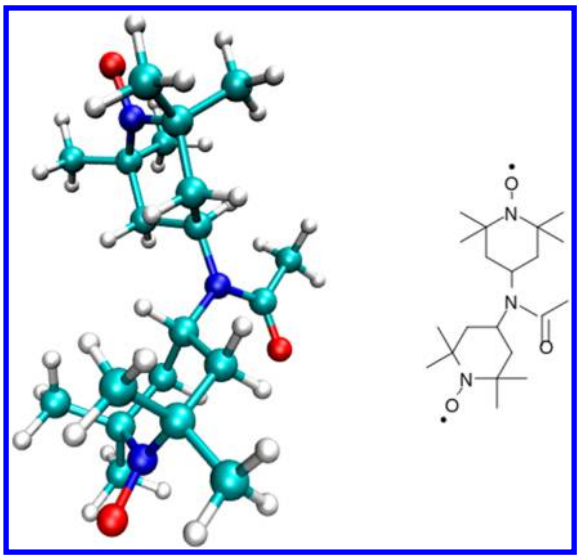

Figure 6. A dinitroxide biradical under investigation for antimicrobial properties. It undergoes a single electron oxidation with a potential of 845 mV vs SHE.[100] Carbon is represented in green, hydrogen in white, nitrogen in blue, and oxygen in red.

because of its structure: it is more globular than our other test molecules and, accordingly, represents a more realistic application. The oxidation potential of the dinitroxide has been measured as 615 mV vs a Ag/AgCl electrode or equivalently 845 mV vs a standard hydrogen electrode (SHE).[100] To compare with experiment, we have computed the oxidation potential using DF-LMRSDCI and DF-LMRACPF2 for the electronic energy. To compute the free energy of the dinitroxide and the corresponding oxidized species, we used the equation

$$G = E_{gas}^{CI} + (G - E)_{gas}^{DFT} + (E_{solm} - E_{gas})^{DFT} + \Delta G^* \quad (13)$$

which has been shown to model redox potentials accurately.[101] E_{gas}^{CI} is the electronic energy at the DF-LMRSDCI/DF-LMRACPF2 level in the gas phase. For the neutral species, a CAS(2,2) was used, containing the two singly occupied orbitals. The singlet and triplet states are degenerate at the CAS(2,2) level as the two unpaired electrons are spatially separated on different rings. The oxidized species required only an ROHF treatment of the remaining singly occupied orbital. $(G-E)_{gas}^{DFT}$ represents the ZPE and thermal contributions calculated with DFT-B3LYP in the gas phase. $(E_{soln}-E_{gas})^{DFT}$ is the solvation correction at the DFT-B3LYP level. We used COSMO to implicitly model the water solvent; no explicit water molecules were used. Finally, ΔG^* accounts for the free energy of the phase change from gas to solute and is equal to 1.89 kcal/mol. For all portions of the calculations, we used the cc-pVDZ basis set and did not scale the vibrational frequencies. We also needed the free energy of an electron to compute the oxidation potential, for which we used the empirical value of 4.281 V for the SHE.[101−103] The final computed oxidation potential (against the SHE electrode) is 663 mV for DF-LMRSDCI and 530 mV for DF-LMRACPF2. The errors compared to experiment, 182 mV and 315 mV, are in the expected range of about 300 mV.[104−106] The DF-LMRACPF2 and DF-LMRSDCI calculations took at most four days of computational time on 16 cores, demonstrating the usefulness of the local correlation and density fitting approximations.

CONCLUSIONS

We incorporated density fitting of the two-electron integrals into our local CI method. The new method, DF-LMRSDCI, has larger errors in total energies compared to our previous method that used Cholesky decomposition, CD-LMRSDCI. However, relative energies computed with DF-LMRSDCI are much more accurate than total energies, allowing the method to be used reliably for applications work. For the systems studied in this work, the accuracy of DF-LMRSCI lies between the accuracies achieved with CD threshold of 10^{-4} and 10^{-5}. This behavior, inaccurate total energies but accurate energy differences, occurs when using DF with other CWs, as well.[96]

We also demonstrated that DF-LMRSDCI is faster than CD-LMRSDCI, at least for the molecules considered here. This is not due to the overall algorithmic scaling, as both methods involve $O(N^4)$ steps. The DF speedup likely has two origins. First, the number of auxiliary basis functions is significantly smaller than the number of Cholesky vectors, at least for accurate CD thresholds. This increases the speed of the AO-to-MO transform and the on-the-fly integral calculation. The smaller number of auxiliary functions is the most important effect. Second, the DF does not involve pivoting, which significantly improves parallelization of the decomposition. The pivoting required in the CD creates a serial bottleneck that does not exist in DF. The second effect is strongly dependent upon the number of threads used throughout the calculation, and the relative speedup of the initial decomposition step with DF compared to CD increases with the number of threads. Finally, we also demonstrated the use of DF-LMRSDCI and DF-LMRACPF2 in a nontrivial molecule, calculating the oxidation potential of a dinitroxide biradical. The oxidation potential compares reasonably with experiment.

There are two logical steps toward improving the use of DF in local CI. First, other local methods use approximate DF methods designed to reduce the $O(N^4)$ scaling of the DF equations. An approximate DF approach will be required to produce a lower scaling algorithm. Second, rewriting the SGGA equations in terms of the decomposed three-index integrals (either DF or CD) would greatly reduce the computational cost by avoiding the expensive on-the-fly recalculation of the four-index integrals.

ASSOCIATED CONTENT

Supporting Information

The Supporting Information is available free of charge on the ACS Publications website at DOI: 10.1021/acs.jctc.5b00762.

Additional timing data, parallel speedups, CPU time overheads, and coordinates of all optimized structures (PDF)

DOI: 10.1021/acs.jctc.5b00762
J. Chem. Theory Comput. 2015, 11, 5242−5251

AUTHOR INFORMATION

Corresponding Author

*Fax: 609 258 5877. E-mail: eac@princeton.edu.

Author Contributions

The manuscript was written through contributions of all authors. All authors have given approval to the final version of the manuscript.

Funding

U.S. National Science Foundation (Grant No. CHE-1265700). Fellowship within the Postdoc-Program of the German Academic Exchange Service (DAAD).

Notes

The authors declare no competing financial interest.

ACKNOWLEDGMENTS

We are grateful for support from the U.S. National Science Foundation (Grant No. CHE-1265700). C.M.K. acknowledges support by a fellowship within the Postdoc-Program of the German Academic Exchange Service (DAAD). All calculations were carried out using Princeton's TIGRESS High Performance Computing resources. We thank Susi Lehtola for providing the ERKALE program, which we used for integral generation, as well as providing helpful discussions and comments.

REFERENCES

(1) Shavitt, I.; Bartlett, R. J. *Many-Body Methods in Chemistry and Physics: MBPT and Coupled-Cluster Theory*, 1st ed.; Cambridge University Press: Cambridge, United Kingdom, 2009.
(2) Bartlett, R. J. *Mol. Phys.* **2010**, *108*, 2905−2920.
(3) Szabo, A.; Ostlund, N. S. *Modern quantum chemistry: introduction to advanced electronic structure theory*, 1st ed.; Macmillan Publishing Co., Inc.: New York, NY, 1982.
(4) Pulay, P. *Chem. Phys. Lett.* **1983**, *100*, 151−154.
(5) Sæbø, S.; Pulay, P. *J. Chem. Phys.* **1987**, *86*, 914−922.
(6) Sæbø, S.; Pulay, P. *Chem. Phys. Lett.* **1985**, *113*, 13−18.
(7) Sæbø, S.; Pulay, P. *Annu. Rev. Phys. Chem.* **1993**, *44*, 213−236.
(8) Sæbø, S.; Pulay, P. *J. Chem. Phys.* **1988**, *88*, 1884−1890.
(9) Schütz, M.; Werner, H.-J. *J. Chem. Phys.* **2001**, *114*, 661−681.
(10) Schütz, M.; Hetzer, G.; Werner, H.-J. *J. Chem. Phys.* **1999**, *111*, 5691−5705.
(11) Maslen, P. E.; Head-Gordon, M. *Chem. Phys. Lett.* **1998**, *283*, 102−108.
(12) Walter, D.; Venkatnathan, A.; Carter, E. A. *J. Chem. Phys.* **2003**, *118*, 8127−8139.
(13) Pisani, C.; Busso, M.; Capecchi, G.; Casassa, S.; Dovesi, R.; Maschio, L.; Zicovich-Wilson, C.; Schütz, M. *J. Chem. Phys.* **2005**, *122*, 094113.
(14) Maschio, L. *J. Chem. Theory Comput.* **2011**, *7*, 2818−2830.
(15) Shao, Y.; Gan, Z.; Epifanovsky, E.; Gilbert, A. T. B.; Wormit, M.; Kussmann, J.; Lange, A. W.; Behn, A.; Deng, J.; Feng, X.; Ghosh, D.; Goldey, M.; Horn, P. R.; Jacobson, L. D.; Kaliman, I.; Khaliullin, R. Z.; Kuś, T.; Landau, A.; Liu, J.; Proynov, E. I.; Rhee, Y. M.; Richard, R. M.; Rohrdanz, M. A.; Steele, R. P.; Sundstrom, E. J.; Woodcock, H. L., III; Zimmerman, P. M.; Zuev, D.; Albrecht, B.; Alguire, E.; Austin, B.; Beran, G. J. O.; Bernard, Y. A.; Berquist, E.; Brandhorst, K.; Bravaya, K. B.; Brown, S. T.; Casanova, D.; Chang, C.-M.; Chen, Y.; Chien, S. H.; Closser, K. D.; Crittenden, D. L.; Diedenhofen, M.; DiStasio, R. A., Jr.; Do, H.; Dutoi, A. D.; Edgar, R. G.; Fatehi, S.; Fusti-Molnar, L.; Ghysels, A.; Golubeva-Zadorozhnaya, A.; Gomes, J.; Hanson-Heine, M. W. D.; Harbach, P. H. P.; Hauser, A. W.; Hohenstein, E. G.; Holden, Z. C.; Jagau, T.-C.; Ji, H.; Kaduk, B.; Khistyaev, K.; Kim, J.; Kim, J.; King, R. A.; Klunzinger, P.; Kosenkov, D.; Kowalczyk, T.; Krauter, C. M.; Lao, K. U.; Laurent, A.; Lawler, K. V.; Levchenko, S. V.; Lin, C. Y.; Liu, F.; Livshits, E.; Lochan, R. C.; Luenser, A.; Manohar, P.; Manzer, S. F.; Mao, S.-P.; Mardirossian, N.; Marenich, A. V.; Maurer, S. A.; Mayhall, N. J.; Neuscamman, E.; Oana, C. M.; Olivares-Amaya, R.; O'Neill, D. P.; Parkhill, J. A.; Perrine, T. M.; Peverati, R.; Prociuk, A.; Rehn, D. R.; Rosta, E.; Russ, N. J.; Sharada, S. M.; Sharma, S.; Small, D. W.; Sodt, A.; Stein, T.; Stück, D.; Su, Y.-C.; Thom, A. J. W.; Tsuchimochi, T.; Vanovschi, V.; Vogt, L.; Vydrov, O.; Wang, T.; Watson, M. A.; Wenzel, J.; White, A.; Williams, C. F.; Yang, J.; Yeganeh, S.; Yost, S. R.; You, Z.-Q.; Zhang, I. Y.; Zhang, X.; Zhao, Y.; Brooks, B. R.; Chan, G. K.-L.; Chipman, D. M.; Cramer, C. J.; Goddard, W. A., III; Gordon, M. S.; Hehre, W. J.; Klamt, A.; Schaefer, H. F., III; Schmidt, M. W.; Sherrill, C. D.; Truhlar, D. G.; Warshel, A.; Xu, X.; Aspuru-Guzik, A.; Baer, R.; Bell, A. T.; Besley, N. A.; Chai, J.-D.; Dreuw, A.; Dunietz, B. D.; Furlani, T. R.; Gwaltney, S. R.; Hsu, C.-P.; Jung, Y.; Kong, J.; Lambrecht, D. S.; Liang, W.; Ochsenfeld, C.; Rassolov, V. A.; Slipchenko, L. V.; Subotnik, J. E.; Van Voorhis, T.; Herbert, J. M.; Krylov, A. I.; Gill, P. M. W.; Head-Gordon, M. *Mol. Phys.* **2015**, *113*, 184−215.
(16) Werner, H.-J.; Manby, F. R.; Knowles, P. J. *J. Chem. Phys.* **2003**, *118*, 8149−8160.
(17) Werner, H.-J.; Schütz, M. *J. Chem. Phys.* **2011**, *135*, 144116.
(18) Lorenz, M.; Usvyat, D.; Schütz, M. *J. Chem. Phys.* **2011**, *134*, 094101.
(19) Venkatnathan, A.; Szilva, A. B.; Walter, D.; Gdanitz, R. J.; Carter, E. A. *J. Chem. Phys.* **2004**, *120*, 1693−1704.
(20) Walter, D.; Szilva, A. B.; Niedfeldt, K.; Carter, E. A. *J. Chem. Phys.* **2002**, *117*, 1982−1993.
(21) Walter, D.; Carter, E. A. *Chem. Phys. Lett.* **2001**, *346*, 177−185.
(22) Chwee, T. S.; Carter, E. A. *J. Chem. Phys.* **2010**, *132*, 074104.
(23) Chwee, T. S.; Szilva, A. B.; Lindh, R.; Carter, E. A. *J. Chem. Phys.* **2008**, *128*, 224106.
(24) Krisiloff, D. B.; Carter, E. A. *Phys. Chem. Chem. Phys.* **2012**, *14*, 7710−7717.
(25) Liakos, D. G.; Hansen, A.; Neese, F. *J. Chem. Theory Comput.* **2011**, *7*, 76−87.
(26) Neese, F.; Hansen, A.; Liakos, D. G. *J. Chem. Phys.* **2009**, *131*, 064103.
(27) Neese, F.; Wennmohs, F.; Hansen, A. *J. Chem. Phys.* **2009**, *130*, 114108.
(28) Yang, J.; Chan, G. K.-L.; Manby, F. R.; Schütz, M.; Werner, H.-J. *J. Chem. Phys.* **2012**, *136*, 144105.
(29) Kitaura, K.; Ikeo, E.; Asada, T.; Nakano, T.; Uebayasi, M. *Chem. Phys. Lett.* **1999**, *313*, 701−706.
(30) Häser, M.; Ahlrichs, R. *J. Comput. Chem.* **1989**, *10*, 104−111.
(31) Lambrecht, D. S.; Ochsenfeld, C. *J. Chem. Phys.* **2005**, *123*, 184101.
(32) Lambrecht, D. S.; Doser, B.; Ochsenfeld, C. *J. Chem. Phys.* **2005**, *123*, 184102.
(33) Maurer, S. A.; Lambrecht, D. S.; Flaig, D.; Ochsenfeld, C. *J. Chem. Phys.* **2012**, *136*, 144107.
(34) Murphy, R. B.; Beachy, M. D.; Friesner, R. A.; Ringnalda, M. N. *J. Chem. Phys.* **1995**, *103*, 1481−1490.
(35) Reynolds, G.; Martínez, T. J.; Carter, E. A. *J. Chem. Phys.* **1996**, *105*, 6455−6470.
(36) Friesner, R. A. *Chem. Phys. Lett.* **1985**, *116*, 39−43.
(37) Beebe, N. H. F.; Linderberg, J. *Int. J. Quantum Chem.* **1977**, *12*, 683−705.
(38) Røeggen, I.; Wisløff-Nilssen, E. *Chem. Phys. Lett.* **1986**, *132*, 154−160.
(39) Koch, H.; Sánchez de Merás, A.; Pedersen, T. B. *J. Chem. Phys.* **2003**, *118*, 9481−9484.
(40) Vahtras, O.; Almlöf, J.; Feyereisen, M. W. *Chem. Phys. Lett.* **1993**, *213*, 514−518.
(41) Hohenstein, E. G.; Parrish, R. M.; Martínez, T. J. *J. Chem. Phys.* **2012**, *137*, 044103.
(42) Neese, F.; Wennmohs, F.; Hansen, A.; Becker, U. *Chem. Phys.* **2009**, *356*, 98−109.
(43) Martínez, T. J.; Carter, E. A. *J. Chem. Phys.* **1995**, *102*, 7564−7572.
(44) Martínez, T. J.; Carter, E. A. *J. Chem. Phys.* **1994**, *100*, 3631−3638.
(45) Martínez, T. J.; Mehta, A.; Carter, E. A. *J. Chem. Phys.* **1992**, *97*, 1876−1880.
(46) Martínez, T. J.; Carter, E. A. *J. Chem. Phys.* **1993**, *98*, 7081−7085.

DOI: 10.1021/acs.jctc.5b00762
J. Chem. Theory Comput. 2015, 11, 5242−5251

(47) Martínez, T. J.; Carter, E. A. *Chem. Phys. Lett.* **1995**, *241*, 490−496.
(48) Hohenstein, E. G.; Kokkila, S. I. L.; Parrish, R. M.; Martínez, T. J. *J. Chem. Phys.* **2013**, *138*, 124111.
(49) Parrish, R. M.; Hohenstein, E. G.; Martínez, T. J.; Sherrill, C. D. *J. Chem. Phys.* **2012**, *137*, 224106.
(50) Parrish, R. M.; Hohenstein, E. G.; Martínez, T. J.; Sherrill, C. D. *J. Chem. Phys.* **2013**, *138*, 194107.
(51) Hohenstein, E. G.; Parrish, R. M.; Sherrill, C. D.; Martínez, T. J. *J. Chem. Phys.* **2012**, *137*, 221101.
(52) Kendall, R. A.; Früchtl, H. A. *Theor. Chem. Acc.* **1997**, *97*, 158−163.
(53) Klopper, W.; Samson, C. C. M. *J. Chem. Phys.* **2002**, *116*, 6397−6410.
(54) Schütz, M.; Manby, F. R. *Phys. Chem. Chem. Phys.* **2003**, *5*, 3349−3358.
(55) Manby, F. R. *J. Chem. Phys.* **2003**, *119*, 4607−4613.
(56) Womack, J. C.; Manby, F. R. *J. Chem. Phys.* **2014**, *140*, 044118.
(57) May, A. J.; Manby, F. R. *J. Chem. Phys.* **2004**, *121*, 4479−4485.
(58) Polly, R.; Werner, H.-J.; Manby, F. R.; Knowles, P. J. *Mol. Phys.* **2004**, *102*, 2311−2321.
(59) Schütz, M.; Werner, H.-J.; Lindh, R.; Manby, F. R. *J. Chem. Phys.* **2004**, *121*, 737−750.
(60) Werner, H.-J.; Manby, F. R. *J. Chem. Phys.* **2006**, *124*, 054114.
(61) Tew, D. P.; Klopper, W.; Neiss, C.; Hättig, C. *Phys. Chem. Chem. Phys.* **2007**, *9*, 1921−1930.
(62) Knizia, G.; Adler, T. B.; Werner, H.-J. *J. Chem. Phys.* **2009**, *130*, 054104.
(63) Bates, J. E.; Shiozaki, T. *J. Chem. Phys.* **2015**, *142*, 044112.
(64) DePrince, A. E., III; Kennedy, M. R.; Sumpter, B. G.; Sherrill, C. D. *Mol. Phys.* **2014**, *112*, 844−852.
(65) Hrenar, T.; Rauhut, G.; Werner, H.-J. *J. Phys. Chem. A* **2006**, *110*, 2060−2064.
(66) Kats, D.; Korona, T.; Schütz, M. *J. Chem. Phys.* **2006**, *125*, 104106.
(67) Aquilante, F.; Gagliardi, L.; Pedersen, T. B.; Lindh, R. *J. Chem. Phys.* **2009**, *130*, 154107.
(68) Chwee, T. S.; Carter, E. A. *Mol. Phys.* **2010**, *108*, 2519−2526.
(69) Epifanovsky, E.; Zuev, D.; Feng, X.; Khistyaev, K.; Shao, Y.; Krylov, A. I. *J. Chem. Phys.* **2013**, *139*, 134105.
(70) DePrince, A. E., III; Sherrill, C. D. *J. Chem. Theory Comput.* **2013**, *9*, 2687−2696.
(71) Boström, J.; Aquilante, F.; Pedersen, T. B.; Lindh, R. *J. Chem. Theory Comput.* **2009**, *5*, 1545−1553.
(72) Hohenstein, E. G.; Sherrill, C. D. *J. Chem. Phys.* **2010**, *132*, 184111.
(73) Krisiloff, D. B.; Dieterich, J. M.; Libisch, F.; Carter, E. A. Numerical Challenges in a Cholesky-Decomposed Local Correlation Quantum Chemistry Framework. In *Mathematical and Computational Modeling With Applications in the Natural and Social Sciences, Engineering, and the Arts*; Melnick, R., Ed.; John Wiley & Sons, Inc.: Hoboken, NJ, 2015; pp 59−91.
(74) Hammarling, S.; Higham, N. J.; Lucas, C. LAPACK-Style Codes for Pivoted Cholesky and QR Updating. In *Applied Parallel Computing. State of the Art in Scientific Computing*; Kågström, B., Elmroth, E., Dongarra, J., Wasniewski, J., Eds.; Lecture Notes in Computer Science; Springer: Berlin/Heidelberg, Germany, 2007; Vol. *4699*, pp 137−146.
(75) The openmp api specification for parallel programming. http://openmp.org/wp (accessed October 1, 2015).
(76) Davidson, E. R. *J. Comput. Phys.* **1975**, *17*, 87−94.
(77) Duch, W.; Karwowski, J. *Comput. Phys. Rep.* **1985**, *2*, 93−170.
(78) Knowles, P. J.; Werner, H.-J. *Chem. Phys. Lett.* **1988**, *145*, 514−522.
(79) Karwowski, J. *J. Math. Chem.* **1998**, *23*, 127−149.
(80) Duch, W.; Karwowski, J. *Theor. Chem. Accounts Theory, Comput. Model. (Theoretica Chim. Acta)* **1979**, *51*, 175−188.
(81) Gdanitz, R. J.; Ahlrichs, R. *Chem. Phys. Lett.* **1988**, *143*, 413−420.
(82) Gdanitz, R. J. *Int. J. Quantum Chem.* **2001**, *85*, 281−300.
(83) Pipek, J.; Mezey, P. G. *J. Chem. Phys.* **1989**, *90*, 4916−4926.
(84) Subotnik, J. E.; Dutoi, A. D.; Head-Gordon, M. *J. Chem. Phys.* **2005**, *123*, 114108.
(85) Oyeyemi, V. B.; Dieterich, J. M.; Krisiloff, D. B.; Tan, T.; Carter, E. A. *J. Phys. Chem. A* **2015**, *119*, 3429−3439.
(86) Dieterich, J. M.; Carter, E. A. *Comput. Theor. Chem.* **2015**, *1051*, 47−56.
(87) Aquilante, F.; De Vico, L.; Ferré, N.; Ghigo, G.; Malmqvist, P.-Å.; Neogrády, P.; Pedersen, T. B.; Pitoňák, M.; Reiher, M.; Roos, B. O.; Serrano-Andrés, L.; Urban, M.; Veryazov, V.; Lindh, R. *J. Comput. Chem.* **2010**, *31*, 224−247.
(88) Neese, F. *Wiley Interdiscip. Rev. Comput. Mol. Sci.* **2012**, *2*, 73−78.
(89) Dunning, T. H., Jr. *J. Chem. Phys.* **1989**, *90*, 1007−1023.
(90) Weigend, F.; Köhn, A.; Hättig, C. *J. Chem. Phys.* **2002**, *116*, 3175−3183.
(91) Hättig, C. *Phys. Chem. Chem. Phys.* **2005**, *7*, 59−66.
(92) Cramer, C. J. *Essentials of Computational Chemistry: Theories and Models*, 2nd ed.; John Wiley & Sons Ltd.: Chichester, West Sussex, United Kingdom, 2004.
(93) Valeev, E. F.; Ferman, J. T. *LIBINT — a library for the evaluation of molecular integrals of two-body operators over Gaussian functions, Version 1.1.6*; Copyright (C) 1996−2014. http://sourceforge.net/p/libint/ (accessed Oct 1, 2015).
(94) Lehtola, J.; Hakala, M.; Sakko, A.; Hämäläinen, K. *J. Comput. Chem.* **2012**, *33*, 1572−1585.
(95) Lehtola, S. *ERKALE — HF/DFT from Hel*; 2014. http//erkale.googlecode.com (accessed Oct 1, 2015).
(96) Aquilante, F.; Lindh, R.; Pedersen, T. B. *J. Chem. Phys.* **2007**, *127*, 114107.
(97) Pedersen, T. B.; Aquilante, F.; Lindh, R. *Theor. Chem. Acc.* **2009**, *124*, 1−10.
(98) Boström, J.; Delcey, M. G.; Aquilante, F.; Serrano-Andrés, L.; Pedersen, T. B.; Lindh, R. *J. Chem. Theory Comput.* **2010**, *6*, 747−754.
(99) Aquilante, F.; Pedersen, T. B.; Lindh, R.; Roos, B. O.; Sánchez De Merás, A.; Koch, H. *J. Chem. Phys.* **2008**, *129*, 024113.
(100) Kavala, M.; Brezová, V.; Švorc, L.; Vihonská, Z.; Olejníková, P.; Moncol, J.; Kožíšek, J.; Herich, P.; Szolcsányi, P. *Org. Biomol. Chem.* **2014**, *12*, 4491−4502.
(101) Keith, J. A.; Carter, E. A. *J. Am. Chem. Soc.* **2012**, *134*, 7580−7583.
(102) Keith, J. A.; Carter, E. A. *Chem. Sci.* **2013**, *4*, 1490−1496.
(103) Isse, A. A.; Gennaro, A. *J. Phys. Chem. B* **2010**, *114*, 7894−7899.
(104) Hughes, T. F.; Friesner, R. A. *J. Phys. Chem. B* **2011**, *115*, 9280−9289.
(105) Baik, M.-H.; Friesner, R. A. *J. Phys. Chem. A* **2002**, *106*, 7407−7412.
(106) Klicić, J. J.; Friesner, R. A.; Liu, S.-Y.; Guida, W. C. *J. Phys. Chem. A* **2002**, *106*, 1327−1335.

DOI: 10.1021/acs.jctc.5b00762
J. Chem. Theory Comput. 2015, 11, 5242−5251